GASEOUS Ni^+ COMPLEXES WITH BINOL DERIVATIVES AND CHIRAL ESTERS IN THE GAS PHASE: AN EXPERIMENTAL AND THEORETICAL INVESTIGATION

Francesca R. NOVARA[a1], Xinhao ZHANG[a2], Detlef SCHRÖDER[b,*] and Helmut SCHWARZ[a3,*]

[a] *Institut für Chemie der Technischen Universität Berlin, Strasse des 17. Juni 135, 106 23 Berlin, Germany; e-mail:* [1] *francesca.novara@mail.chem.tu-berlin.de,* [2] *xinhao.zhang@mail.chem.tu-berlin.de,* [3] *helmut.schwarz@mail.chem.tu-berlin.de*

[b] *Institute of Organic Chemistry and Biochemistry, Academy of Sciences of the Czech Republic, v.v.i., Flemingovo nám. 2, 166 10 Prague 6, Czech Republic; e-mail: detlef.schroeder@uochb.cas.cz*

Received August 5, 2008
Accepted October 30, 2008
Published online February 14, 2009

The gas-phase behavior of monocationic Ni(II) complexes that contain as building blocks optically pure BINOL derivatives and two chiral hydroxy esters is investigated by means of electrospray ionization (ESI) mass spectrometry. Upon collision-induced dissociation (CID), the complexes containing ethyl 2-hydroxypropionate (ethyl lactate) only lose the ester ligand. The complexes bearing ethyl 3-hydroxybutyrate instead either lose the ester ligands or undergo bond activation followed by elimination of the corresponding β-ketoester (ethyl acetylacetate) as revealed by deuterium labeling. Comparison of the results obtained for complexes with different chiralities reveals the operation of a significant stereochemical effect (*SE*) in the gas-phase dehydrogenation of ethyl 3-hydroxybutyrate by gaseous $[(BINOLato)Ni]^+$ ions. Instead, no substantial differences in the CID patterns for the complexes bearing the ester-substituted BINOL derivative are found. The results provide insights into the gas-phase coordination of metal cations by BINOL derivatives and into the molecular features, which are responsible for gas-phase enantioselective processes. Additional mechanistic aspects are disclosed by exploratory calculations employing density functional theory using the B3LYP method.

Keywords: BINOL; Enantioselectivity; Ethyl butyrate; Ethyl lactate; Mass spectrometry; Nickel; Binaphthyls; Binaphthols; Collision-induced dissociation; DFT calculations.

Despite the wide applications of BINOL (1,1′-bi-2-naphthol) and its derivates in asymmetric synthesis[1], the mechanistic understanding of the role of such ligands in chiral induction is still limited. In this respect, gas-phase studies can provide molecular insight how certain reactions can be favored or suppressed for one or the other enantiomer of a given substrate[2–4]. Recent mass-spectrometric experiments have addressed the behavior of

doi:10.1135/cccc2008168

complexes between transition metals and BINOL ligands[5,6]. In particular, significant chiral effects in bond-activation processes have been observed in the gas phase. To this end, chiral secondary alcohols have been added to chiral nickel complexes to yield complexes of the composition $[(BINOLato)Ni(CH_3(CH(OH))R)]^+$, where BINOLato refers to the singly deprotonated BINOL [7,8]. Collision-induced dissociation (CID) of these complexes resulted in two competing fragmentation channels: the loss of the entire alkanol ligand and the elimination of the corresponding ketone, obtained upon bond activation at the chiral center of the secondary alcohol. The branching ratios (BRs) of these two channels for both diastereomers of the complexes provided a measure of the chiral effect operative in the gas-phase dehydrogenation of the secondary alcohols. Using "Cook's kinetic method"[9], the ligand-loss channel has instead been proven to bear a negligible stereochemical effect for the systems investigated and can therefore serve as an internal standard. The application of this method to mass selected $[(BINOLato)Ni]^+$ complexes bound to a series of secondary alcohols has furnished small, yet considerable stereochemical effects (*SE*s) with preferential bond activation for the homochiral complexes. In the case of aromatic alcohols, however, significant stereoselectivity in the opposite direction was found. An extension of these studies to complexes bearing different chiral auxiliaries and modified substrates offers a systematic approach towards understanding the structural features, which are responsible for the induction of chiral effects in bond-activation processes. Particular interest in stereoselective dehydrogenation of alcohols arises from the considerable role of the reverse reaction, i.e. asymmetric hydrogenation of ketones, in organic synthesis, which are are often catalyzed by BINOL-containing metal complexes[10] similar to the systems of our present study.

In this work, we report on the gas-phase generation and reactivity of Ni(II) complexes containing the singly deprotonated form of BINOL or [(1,1′-bisnaphthalene)-(3,3′-dicarboxylic acid)-2,2′-dihydroxy-dimethyl ester], compounds **1** and **2** in Scheme 1 as the chiral ligand, and the hydroxy-esters ethyl 2-hydroxypropionate (ethyl lactate, **3**) and ethyl 3-hydroxy-butyrate (**4**) as the chiral substrates for bond activation. The choice of **2**, bearing the "bulky" methyl ester groups was motivated by the assumption that a more hindered environment around the charged metal center might induce a higher selectivity. Furthermore, the presence of the carboxy-methyl moieties, offering additional coordination sites, could favor the formation of the complexes upon ESI [11]. Along this line of reasoning, hydroxy esters have been chosen because of putatively chelating coordination to the metal. The previous investigations of aliphatic alcohols revealed negligible

or only moderate enantioselectivities with (BINOLato)Ni^+ cations[7,8], most probably because the carbon backbone is too loosely bound to the active metal site. The presence of an additional coordination site in the substrate might therefore make the systems more rigid and thereby possibly increase the desired enantioselective effects. Note that short-chain esters of hydroxycarboxylic acids are involved in a large number of biological processes and also play a significant role as chiral auxiliaries in asymmetric synthesis[12–14].

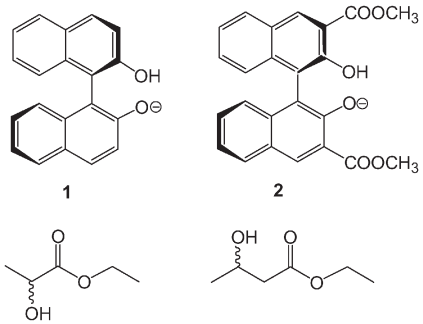

SCHEME 1

EXPERIMENTAL

The mass spectrometric experiments were performed with a commercial VG BIO-Q mass spectrometer described elsewhere[15]. Briefly, the VG BIO-Q consists of an ESI source combined with a tandem mass spectrometer of QHQ configuration (Q stands for quadrupole and H for hexapole). In the present experiments, mmolar methanolic solutions of nickel(II) nitrate, optically pure **1** and **2**, respectively, and one of the chiral esters **3** and **4** were introduced via a syringe pump (flow rate ca. 3 μl/min) to the fused-silica capillary of the ESI source. N_2 was used as drying and nebulizing gas at a source temperature of 80 °C. The instrument parameters have been optimized for maximal abundances of the ions of interest and kept constant for each diastereomeric couple. The best yields have been achieved by optimizing the cone voltage U_C in the range of 40–60 V. The stoichiometric identity of all complexes was confirmed by comparison with the expected isotope patterns[16] in either the ion-source spectra or in appropriate neutral-loss scans[17]. For CID, the ions of interest were mass-selected using the first quadrupole Q1, and interacted with xenon as a collision gas in the hexapole H at various collision energies (E_{lab} = 0–25 eV) at a pressure of about 3.0×10^{-4} mbar; the latter approximately corresponds to single-collision conditions[15]. The product ions formed were then monitored by scanning Q2; in all MS and MS/MS experiments, a good unit-mass resolution of both Q1 and Q2 was adjusted such that ions differing by Δm = ±1 amu can be distinguished safely.

The laboratory collision energies in CID are converted to the center-of-mass frame, $E_{CM} = [m/(M + m)]E_{lab}$, in which m and M are the masses of the collision gas and the ionic species, respectively. Variation of the collision energy leads to breakdown diagrams which permit the determination of phenomenological appearance energies (*AE*s) of the fragmentation channels by linear extrapolation of the signal onsets to the baseline[18]. The errors of the *AE*s

are estimated by applying different linear extrapolations, which are still in reasonable agreement with the experimental data. As pointed out previously[15], the VG BIO-Q is not equipped with differential pumping in the analyzer region, and consequently the collision gas may not only be present in the hexapole collision cell, but also in the focusing region between the mass analyzers. Therefore, the *AE*s reported below do not correspond to the true thermodynamic thresholds, but are only proportional to them. Nevertheless, previous work has established that this method provides approximate energetics, which are fairly sufficient for most mechanistic discussions[19–23].

An exploratory computational study of some relevant intermediates and transition states employed density functional theory (DFT) using the B3LYP hybrid functional method implemented in the Gaussian 03 package[24]. With regards to the basis sets, the geometries have been optimized using Lanl2DZ with *f* polarization functions for nickel[25], while 6-31G** basis sets were employed for all other elements. Frequency calculations were carried out on all the optimized structures with the same method to confirm the stationary points on the potential-energy surface and to obtain the zero-point energy as well as the free energy corrections at 298.15 K. In the discussion, only the relative free energies are presented. In terms of model systems, compounds *R*-**1**, *S*-**3**, and *S*-**4** have been computed as such, whereas compound *R*-**2′** is used as a model of *R*-**2** (Scheme 4) in order to reduce the size and the conformational space.

RESULTS AND DISCUSSION

Electrospray ionization of a solution of nickel(II) salts and a bisnaphthol in methanol leads to abundant cations of the type $[(\text{BINOLato})\text{Ni}(\text{CH}_3\text{OH})_n]^+$ in which the Ni(II) is coordinated to a singly deprotonated bisnaphtholato ligand with additional coordination by solvent molecules. In the presence of larger alcohols or other suitable compounds, the methanol ligands can be replaced by these substrate molecules. Accordingly, combination of the BINOL-type ligands and the hydroxy esters leads to four different Ni(II) complexes, all of which have been investigated with both chiralities of the bisnaphthol and the hydroxy esters.

Ni-BINOLato Complexes of Ethyl Lactate

Upon ESI of a ternary mixture of BINOL, $Ni(NO_3)_2$, and ethyl lactate (**3**), complexes of the type $[(\text{BINOLato})\text{Ni}(\mathbf{3})]^+$ are formed in good yields. The CID spectra of mass-selected $[(R\text{-}\mathbf{1})\text{Ni}(S\text{-}\mathbf{3})]^+$ complexes (*m/z* 461) were investigated as a function of collision energies ranging from E_{lab} = 0 to 25 eV. In the entire range of collision energies and for all four possible combinations of chiralities of the components, i.e. $[(R\text{-}\mathbf{1})\text{Ni}(R\text{-}\mathbf{3})]^+$, $[(R\text{-}\mathbf{1})\text{Ni}(S\text{-}\mathbf{3})]^+$, $[(S\text{-}\mathbf{1})\text{Ni}(R\text{-}\mathbf{3})]^+$, and $[(S\text{-}\mathbf{1})\text{Ni}(S\text{-}\mathbf{3})]^+$, the only fragmentation observed leads to a peak at a mass-to-charge ratio *m/z* 343, which is assigned to the loss of the entire ester ligand as a neutral fragment (reaction (*1*)).

$$[(\text{BINOLato})\text{Ni}(\mathbf{3})]^+ \rightarrow [(\text{BINOLato})\text{Ni}]^+ + \mathbf{3} \qquad (1)$$

From Fig. 1a, an appearance energy of $AE_{461\rightarrow343}$ = (1.1 ± 0.2) eV for the loss of ethyl lactate is derived. This value is similar to what has been found previously for the elimination of 1-phenylethanol from $[(\text{BINOLato})\text{Ni}]^+$ complexes; the thresholds for the evaporation of aliphatic 2-alkanols from their $[(\text{BINOLato})\text{Ni}]^+$ complexes are considerably lower, e.g. (0.6 ± 0.2) eV

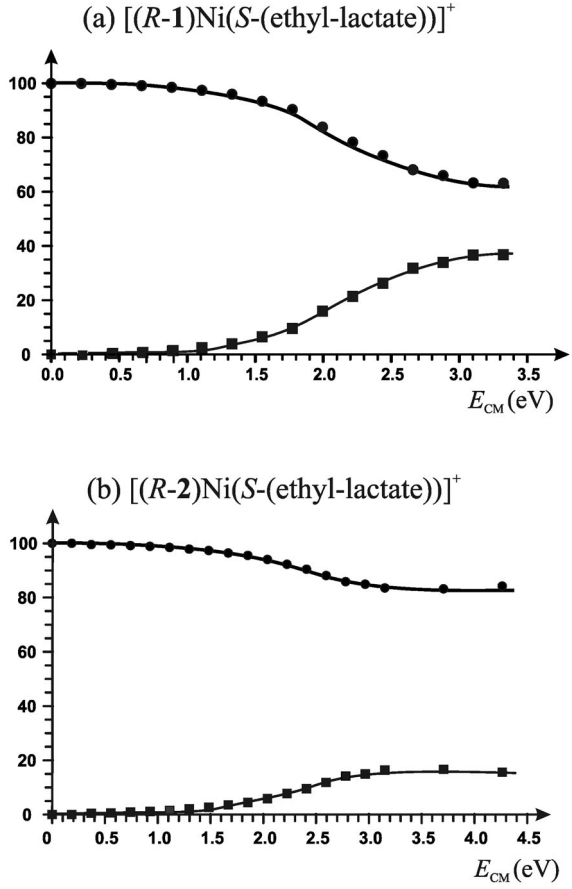

FIG. 1

Breakdown graphs for the CID of mass-selected a $[(R\text{-}\mathbf{1})\text{Ni}(S\text{-}\mathbf{3})]^+$ (*m/z* 461) and b $[(R\text{-}\mathbf{2})\text{Ni}(S\text{-}\mathbf{3})]^+$ (*m/z* 577) showing the abundances of the parent ions (both ●) and the bare bisnaphtholato fragments a $[(R\text{-}\mathbf{1})\text{Ni}]^+$ (*m/z* 343) and b $[(R\text{-}\mathbf{2})\text{Ni}]^+$ (*m/z* 459), respectively (both ■), as a function of the collision energy in the center-of-mass frame

for 2-octanol[8]. In the case of 1-phenylethanol, the larger value was considered as an indication for the interaction of the nickel center with the aromatic ring of the backbone[26–28]. Likewise, comparison of the *AE*s points to the occurrence of an interaction between nickel and both the hydroxy and the carboxy group of the substrate molecule in the cation [(*R*-**1**)Ni(*S*-**3**)]$^+$ consisting of [(*R*-BINOLato)Ni]$^+$ and *S*-ethyl lactate.

Theoretical studies employing density functional theory lend further support to these conclusions. Thus, the most stable configuration of the possible forms of [(*R*-**1**)Ni(*S*-**3**)]$^+$ bears a tetra-coordinated nickel center involving the two oxygen atoms of the BINOL, the hydroxy group of the substrate and the carbonyl oxygen of the ester unit (Scheme 2). Comparison with the corresponding complex of isopropanol points to an additional stabilization of about 0.7 eV (65 kJ/mol) due to the presence of the ester function. There are three possibilities for the coordination to **3**, which are $O_{hydroxyl}$, $O_{carbonyl}$, and O_{ether}. All these possibilities have been taken into account and the most stable one, as depicted in Scheme 2, utilizes $O_{carbonyl}$ and $O_{hydroxyl}$.

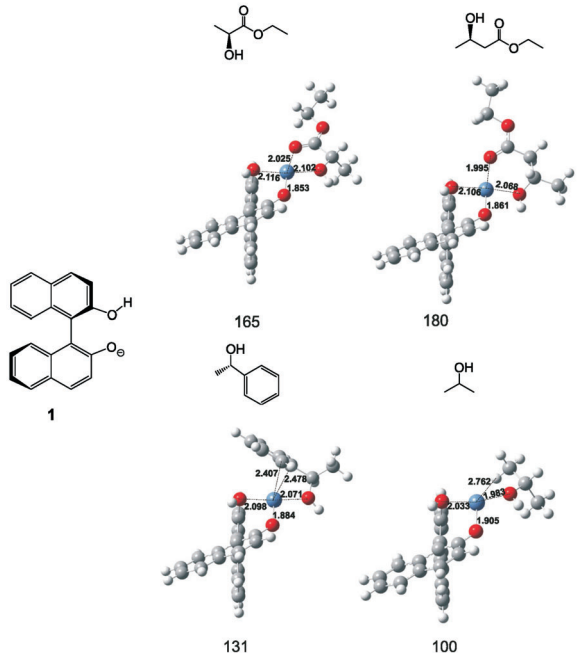

SCHEME 2

Optimized geometries of the [(**1**)Ni]$^+$ complexes with different alcohol ligands (ROH); the structures refer to the most stable isomers. The binding energies relative to [(**1**)Ni]$^+$ + ROH are given in kJ/mol and the distances in Å

This type of coordination is favored because the carbonyl moiety is a very good donor ligand, and further stability is gained from the coordination to the hydroxyl group leading to a five-membered ring. Probably due to competition of the various coordination sites in the modified bisnaphthol ligand **2** bearing a carboxymethyl substituent in the ortho-position, the corresponding $AE_{577\rightarrow459}$ = (1.3 ± 0.2) eV for the loss of ethyl lactate from [(*R*-**2**)Ni(*S*-**3**)]$^+$ is somewhat greater than $AE_{461\rightarrow343}$ = (1.1 ± 0.2) eV (Fig. 1b). Also in this case, no fragmentation channels other than the loss of the intact hydroxy ester ligands are observed and the results are identical for all different combinations of chiralities. While there might in fact exist a small effect of chirality on the appearance energies in CID [29], this is expected to be insignificant for the present systems, because the energy difference of the various diastereomeric ions, e.g. homochiral [(*R*-**2**)Ni(*R*-**3**)]$^+$ versus heterochiral [(*R*-**2**)Ni(*S*-**3**)]$^+$, is expected to be much smaller than the magnitude of the *AE* itself and also most likely lower than the experimental uncertainties of about ΔAE = ±0.2 eV. Therefore, the [(BINOLato)Ni]$^+$ complexes of ethyl lactate cannot be used for the investigation of chiral effects in the gas phase with the methods employed.

Ni-BINOLato Complexes of Ethyl 3-Hydroxybutyrate

The scenario is quite different if the ethyl ester of hydroxybutyric acid is used in which the hydroxy and ester functions are separated by a methylene group. Like in the case of ethyl lactate, the most abundant fragment at *m/z* = 343 in the CID spectrum of mass-selected [(*R*-**1**)Ni(*S*-ethyl 3-hydroxybutyrate)]$^+$ corresponds to the loss of the entire ester ligand (reaction (*2*)). However, another peak appears two mass units higher at *m/z* = 345 (Fig. 2). Based on our previous studies of [(BINOLato)Ni]$^+$ complexes[8], the uptake of two hydrogen atoms by this fragment indicates the dehydrogenation of the alcohol to the corresponding carbonyl compound, i.e. ethyl acetylacetate concomitant with formation of a nickel-hydrido species (reaction (*3*)).

$$[(\text{BINOLato})\text{Ni}(\mathbf{4})]^+ \rightarrow [(\text{BINOLato})\text{Ni}]^+ + \mathbf{4} \qquad (2)$$

$$\rightarrow [(\text{BINOL})\text{NiH}]^+ + CH_3COCH_2COOC_2H_5 \qquad (3)$$

In order to clarify the regioselectivity of the formal dehydrogenation according to reaction (*3*), the corresponding experiments using the labeled (racemic) ethyl 3-hydroxybutyrates **4a**–**4d** shown in Scheme 3 have been performed (Table I).

Table I shows that CID of the complexes of $[(\mathbf{1})Ni]^+$ with **4b** and **4d** leads exclusively to peaks at *m/z* 343 and 345, indicating that no deuterium has been incorporated in the ionic products. In contrast, CID of $[(\mathbf{1})Ni(\mathbf{4a})]^+$ with the substrate deuterated at C(3) affords signals at *m/z* 343 and 346. The mass shift of the latter fragment by Δm = +1 indicates the selective transfer of H(D) from the 3-position of the ester ligand. Further, the shift of the bond-activation product to *m/z* 348 upon CID of mass-selected $[(\mathbf{1})Ni(\mathbf{4c})]^+$ shows that there is also H(D) migration from the hydroxy moiety; note that in this case also the remaining hydroxy group of the BINOLato ligand is deuterated by CH_3OD used as a solvent. Similarly to the results obtained for secondary alcohols[8], it can thus be concluded that the bond activation of ethyl 3-hydroxybutyrate upon CID of its complexes with $[(\mathbf{1})Ni]^+$ as well $[(\mathbf{2})Ni]^+$ leads to the corresponding β-ketoester, i.e. ethyl acetylacetate, as already indicated in reaction (*3*). The latter is produced via dehydrogenation of the secondary alcohol concomitant with the uptake of two hydrogen atoms by the Ni complex.

Based on the experimental observations, a conceivable mechanism for this bond-activation process and the relevant potential-energy surface (PES) have been investigated by means of quantum chemical calculations. The reaction between the d^8 Ni(II) complex $[(\mathbf{1})Ni]^+$ and *S*-ethyl 3-hydroxy-

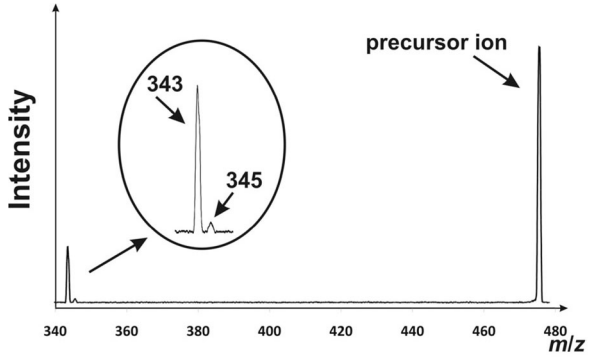

FIG. 2
CID spectrum of mass-selected [(*R*-BINOLato)Ni(*S*-ethyl 3-hydroxybutyrate)]$^+$ (*m/z* 475) at a collision energy of E_{lab} = 7 eV

butyrate can proceed in the singlet and triplet state, which have both been considered (Fig. 3). While triplet states are more stable throughout the PES, the state splitting is moderate and sometimes even quite small. As the gap between the two PESs depicted in Fig. 3 reflects the influence on the binding of the ligands to the nickel in the different spin states, it can be concluded that the preference for the triplet state increases with a decreasing number of coordinating ligands. In line with this reasoning, the singlet and triplet states are almost isoenergetic for structure **8** in which the nickel atom can potentially interact with five ligands, i.e. the two oxygen atoms

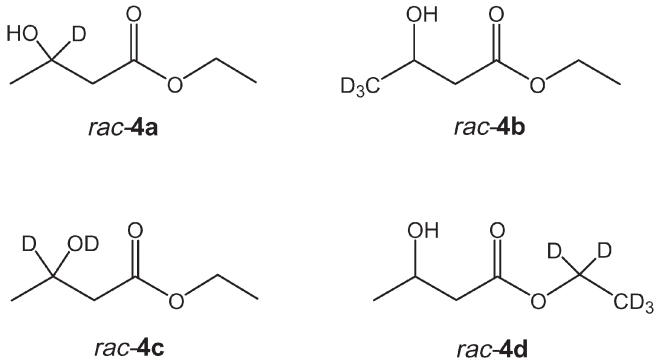

SCHEME 3

TABLE I

Mass-to-charge ratios (*m*/*z*) of the signals due to ligand loss (reaction (*2*)) and bond activation (reaction (*3*)) obtained upon CID of mass-selected [(BINOLato)Ni(**4**)]$^+$ complexes and the isotopologues [(BINOLato)Ni(**4a**–**4d**)]$^+$ at a collision energy of E_{lab} = 10 eV [a,b]

Alcohol	*m*/*z* ligand loss		*m*/*z* bond activation		
	343	344	345	346	348
4	91		9		
4a	88			12	
4b	87		13		
4c[c]		90			10
4d	87		13		

[a] Data normalized to a sum of 100. [b] Similar results were obtained with the corresponding complexes [(**2**)Ni(**4a**–**4d**)]$^+$ (not shown). [c] This complex was measured using CH_3OD as a solvent, which also leads to H/D exchange of the remaining [OH]-proton of the BINOLato ligand resulting in an additional shift of the fragment ions by Δm = +1.

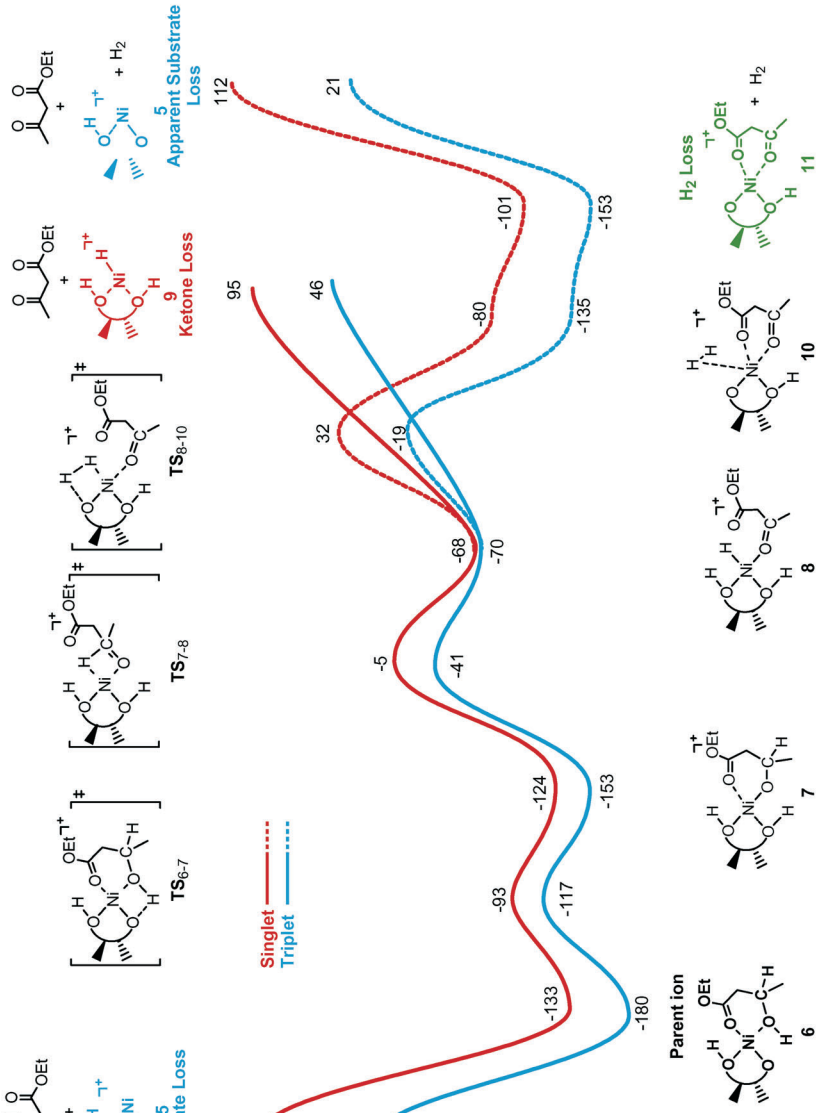

FIG. 3
Calculated potential-energy surface of the dehydrogenation pathway for [(*R*-**1**)Ni(*S*-ethyl 3-hydroxybutyrate)]$^+$. Free reaction energies (at 298 K) are given in kJ/mol relative to separated [(*R*-**1**)Ni]$^+$ + *S*-ethyl 3-hydroxybutyrate

of the BINOL, the two carbonyl groups of the preformed product, and the hydrido ligand. However, because the triplet PES is always lower in energy, the following discussion is focused on the triplet states.

Closer inspection of Fig. 3 has several implications. Structure **6** is the most stable species on the PES. Loss of the intact ligand requires a dissociation energy of 180 kJ/mol, which is consistent with the experimental *AE* = (1.5 ± 0.2) eV (see below). Proton transfer from the hydroxy group of the ester to the anionic oxo ligand of the BINOLate leads to the alternative alkoxo structure [(BINOL)NiOR]$^+$, **7**. The overall reaction **6** → **7** is slightly endothermic and the respective transition structure $\mathbf{TS_{6\text{-}7}}$ is associated with a barrier of 63 kJ/mol (relative to **6**). The energy difference of 27 kJ/mol in favor of **6** thus supports the intuitive assignment of **6**, rather than **7**, as the parent ion[5,7,8]. Moreover, structure **6** is the most stable species on the entire section of the PES studied here, and racemization via reversible C–H bond-activation steps is hence unlikely to occur. The C–H bond activation proceeds via $\mathbf{TS_{7\text{-}8}}$, which represents the rate-determining step en route to the ketone complex **8**. In this transition structure, the carbonyl group of the bidentate ester ligand is released, thereby providing a vacant site for the reaction to occur. The relative free energy of $\mathbf{TS_{7\text{-}8}}$ is –41 kJ/mol in comparison to the entrance channel, which corresponds to a barrier of 139 kJ/mol from the parent ion **6**. From the following intermediate **8**, the ketone can be lost as a neutral molecule upon CID as observed experimentally. The ionic product of this dissociation, complex **9**, is located 46 kJ/mol above the reference channel due to [(**1**)Ni]$^+$ + **2**, which is consistent with the ca. 1:10 ratio of ketone and ligand losses observed in the experimental data (Table I). The hydrido ligand in **8** can also couple with an [OH]-proton of the BINOL ligand to form molecular hydrogen (dashed pathway in Fig. 3, reaction (*4*)). The formation of H_2 and the re-coordination of the ester carbonyl oxygen induce a large driving force for this step. In intermediate **10**, the dihydrogen molecule is only very weakly bound to the Ni center and its evaporation is an entropically favored process (hence ΔG is even negative, Fig. 3). We note in this context that for the system [(**2**)Ni(ethyl 3-hydroxybutyrate)]$^+$, the cationic intermediate corresponding to **11** is detected as an H_2-loss channel (see below). The subsequent loss of the ketone ligand from **11** requires 174 kJ/mol. The product results in [(**1**)Ni]$^+$, which coincides with ligand loss in the mass spectrometric experiments and therefore is labeled as "apparent substrate loss". In this channel, [(**1**)Ni]$^+$ formally acts as a catalyst for the dehydrogenation of *S*-ethyl 3-hydroxybutyrate to ethyl acetylacetate (reaction (*5*)), which is computed to be endothermic by 21 kJ/mol.

$$[(\text{BINOLato})\text{Ni}(\mathbf{4})]^+ \rightarrow \mathbf{11} + \text{H}_2 \qquad (4)$$

$$\text{CH}_3\text{CHOHCH}_2\text{COOC}_2\text{H}_5 \rightarrow \text{CH}_3\text{COCH}_2\text{COOC}_2\text{H}_5 + \text{H}_2 \qquad (5)$$

The computed PES thus provides a rationale for the experimentally observed energy behavior as well as the labeling data (Table I). Until about reaching the threshold for ligand loss, bond activation via $\mathbf{TS_{7\text{-}8}}$ might occur to some extent, but the system prefers to reside in the global minimum **6**. Only above threshold for ligand loss, the ketone ligand in **8** can be expelled to yield the ionic product $[(\text{BINOL})\text{NiH}]^+$ according to reaction (*3*). While the alternative loss of H_2 via $\mathbf{TS_{8\text{-}10}}$ might occur from a mere energetical point of view, it apparently cannot compete with ion dissociation due to the entropic restrictions associated with rearrangement reactions compared to direct bond cleavages. Moreover, once $\mathbf{TS_{8\text{-}10}}$ is passed, the primary product ion **11** contains a considerable amount of internal energy and might hence continue fragmentation to afford $[(\text{BINOLato})\text{Ni}]^+$; a process which might be covered in the ligand-loss channel[30–33]. The agreement between the theoretical and experimental findings is further proven by the comparison of the computed PES with the energy dependencies of competing fragmentations upon CID of the related system $[(\mathbf{2})\text{Ni}(\mathbf{4})]^+$.

Figure 4 shows the competing CID fragmentations observed for mass-selected $[(R\text{-}\mathbf{2})\text{Ni}(R\text{-}\mathbf{4})]^+$. The differences between the complexes of ethyl 3-hydroxybutyrate with $[(R\text{-}\mathbf{1})\text{Ni}]^+$ and $[(R\text{-}\mathbf{2})\text{Ni}]^+$ can serve as a measure for the effect of the carboxymethyl groups on the BINOL ligand. In fact, the ligand loss from $[(R\text{-}\mathbf{2})\text{Ni}(R\text{-}\mathbf{4})]^+$ bears a threshold of (1.8 ± 0.2) eV and reaches an intensity maximum at about 3.6 eV, whereas ligand loss from the complex $[(R\text{-}\mathbf{1})\text{Ni}(S\text{-}\mathbf{4})]^+$ has an apparent threshold of only (1.5 ± 0.2) eV. Accordingly, the ester ligand is more strongly bound to the metal center in $[(\mathbf{2})\text{Ni}]^+$ than in the case of $[(\mathbf{1})\text{Ni}]^+$. In both systems, the ligand-loss channels show a continuous increase with the collision energy, indicating that they do not involve structural rearrangements, but represent simple, continuously endothermic processes. In contrast, the activation channels rise less steeply and flatten out earlier, pointing to the occurrence of entropically demanding pathways such as structural rearrangements. For the system containing $[(\mathbf{2})\text{Ni}]^+$, the loss of H_2 in analogy to reaction (*4*) even outweighs that of the diketone (reaction (*3*)), whereas H_2-loss is not experimentally observed for the complexes of $[(\mathbf{1})\text{Ni}]^+$.

For both BINOLato-type ligands, the C–H bond activation leads to nickel-hydride complexes of the formal composition $[(\mathbf{1}+H)NiH]^+$, and $[(\mathbf{2}+H)NiH]^+$, respectively, which resemble the hydrogenated catalysts in the reduction of ketones with metal hydrides. The systems under investigation can thus be regarded as a gas-phase model for this important class of reactions[8]. By changing the chirality of the components in successive experiments, it is thus possible to probe the chiral effects associated with this reaction. As a measure for a possible *SE*, for the system $[(\mathbf{1})Ni(\mathbf{4})]^+$, we consider the branching ratio between the ligand-loss channel and the evaporation of the correspondent β-ketoester for the different diastereomeric complexes investigated. Previous studies showed that a possible chiral effect in these systems is most likely detected at low collision energies[5]. In this energy range, CID of $[(\mathbf{1})Ni(\mathbf{4})]^+$ does not lead to a significant amount of H_2-loss (reaction (*4*)), whereas CID of the analogous $[(\mathbf{2})Ni(\mathbf{4})]^+$ complexes lose a significant amount of H_2 already at low collision energies. For the latter complexes, the ratio between the ligand-loss channel and the sum of the intensities for the two bond-activation channels for different diastereomeric complexes is therefore considered as a measure of the *SE*. This approximation is based on the assumption that the rate-determining step of the dehydrogenation corresponds to the hydrogen migration from

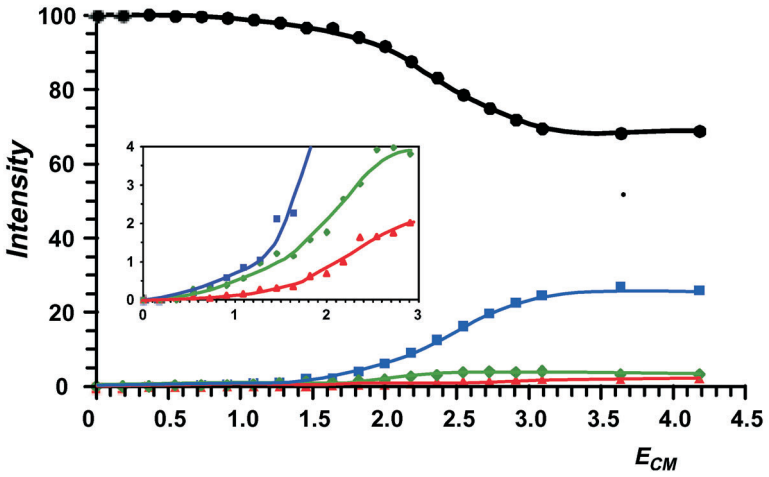

FIG. 4
Breakdown graph of the CID fragments of $[(R\text{-}\mathbf{2})Ni(R\text{-ethyl 3-hydroxybutyrate})]^+$ as a function of collision energy in the center-of-mass frame (black: parent ion, blue: ligand-loss, green: H_2 loss, red: diketone loss)

the ester ligand to the metal center as confirmed by the quantum mechanical calculations discussed above.

In Tables II and III, the relative amounts of the competing fragmentation channels obtained upon CID of the mass-selected BINOLato complexes of $[(R\text{-}\mathbf{1})Ni]^+$ and $[(R\text{-}\mathbf{2})Ni]^+$ with *R*- and *S*-ethyl 3-hydroxybutyrate, respectively, are given. In the last columns, the stereochemical effects derived from the comparison of the diastereomeric pairs are displayed. In the case of ligand **2**, the data does not reveal any significant discrimination (averaged *SE* = 1.10 ± 0.09), whereas a clearly significant effect is observed for the complexes of $[(\mathbf{1})Ni]^+$ (averaged *SE* = 1.41 ± 0.13). A further proof for the measured *SE* is the similar value (1.38 ± 0.12) obtained in analogous CID experiments for the complexes of $[(R\text{-}\mathbf{1})Ni]^+$ with *R*- or *S*-ethyl

TABLE II

Intensities of the fragments due to ligand loss (reaction (*2*)) and C–H bond activation concomitant with the loss of the corresponding β-ketoester (reaction (*3*)) upon CID of mass-selected complexes of $[(R\text{-}\mathbf{1})Ni]^+$ with *R*- and *S*-ethyl 3-hydroxybutyrate, respectively, at variable collision energies (E_{lab} in eV, collision gas: xenon) and the stereochemical effects (*SE*) derived thereof[a]

Complex	E_{lab}	Ligand loss	Bond activation	*SE*[b]
$[(R\text{-}\mathbf{1})Ni(R\text{-}\mathbf{4})]^+$	2	89.1	10.9	1.40 ± 0.07
	3	87.0	13.0	1.67 ± 0.08
	4	90.4	9.6	1.37 ± 0.07
	5	90.2	9.8	1.35 ± 0.07
	6	91.4	8.6	1.30 ± 0.06
	8	92.7	7.3	1.35 ± 0.07
$[(R\text{-}\mathbf{1})Ni(S\text{-}\mathbf{4})]^+$	2	85.4	14.6	
	3	80.0	20.0	
	4	87.3	12.7	
	5	87.2	12.8	
	6	89.1	10.9	
	8	90.4	9.6	

[a] Branching ratios (BR) derived from repeated experiments and normalized to $\sum = 100$. [b] Stereochemical effects defined as $SE = [BR(\mathbf{2})/BR(\mathbf{3})]_{homo}/[BR(\mathbf{2})/BR(\mathbf{3})]_{hetero}$, where the indices "homo" and "hetero" indicate the homochiral (*R*,*R*) and heterochiral (*R*,*S*) complexes with the first indicator assigning the chirality of the BINOL derivative and the second one the chirality of the ester.

3-hydroxypropionate. A comparison of these findings with the results obtained for the secondary aliphatic alcohols[8] confirms the previous suggestion that alcohols which bear an additional coordination site exhibit more pronounced *SE*s.

The origin of such a small, yet considerable selectivity has been theoretically investigated. Although the precise quantification of the chiral effect in terms of energetic differences is beyond the accuracy of the method employed, the stereo-determining transition structures provide insight into the understanding of the experimental observations. According to the PES shown in Fig. 3, the C–H bond activation via transition structure $\mathbf{TS_{7\text{-}8}}$ corresponds to the rate-determining step for the formation of the ketone complexes. In competition with the ligand-loss channel, $\mathbf{TS_{7\text{-}8}}$ hence discriminates the chiral substrates. In the computed structures of $\mathbf{TS_{7\text{-}8}}$ and $\mathbf{TS_{7\text{-}8}}'$ (Fig. 5), the nickel(II) adopts a quasi square planar geometry, while the additional coordination of the metal by the carbonyl group of ethyl 3-hydroxybutyrate has to be released in order to provide a vacant site for the newly forming Ni–H bond.

Table III
Intensities of the fragments due to ligand loss and C–H bond activation concomitant with the losses of the corresponding β-ketoester and H_2 upon CID of mass-selected complexes of $[(R\text{-}\mathbf{2})Ni]^+$ with *R*- and *S*-ethyl 3-hydroxybutyrate, respectively, at variable collision energies (E_{lab} in eV, collision gas: xenon) and the stereochemical effects (*SE*) derived thereof[a]

Complex	E_{lab}	Ligand loss	Bond activation	*SE*[b]
$[(R\text{-}\mathbf{2})Ni(R\text{-}\mathbf{4})]^+$	4	50.0	50.0	1.02 ± 0.05
	5	53.6	46.4	1.09 ± 0.05
	6	54.3	45.7	1.22 ± 0.06
	8	58.3	41.7	1.07 ± 0.05
$[(R\text{-}\mathbf{2})Ni(S\text{-}\mathbf{4})]^+$	4	49.5	50.5	
	5	51.3	48.7	
	6	49.3	50.7	
	8	56.6	43.4	

[a] Branching ratios (BR) derived from repeated experiments and normalized to $\Sigma = 100$. [b] Stereochemical effects defined as $SE = [BR(\mathbf{2})/(BR(\mathbf{3}) + BR(\mathbf{4}))]_{homo}/[BR(\mathbf{2})/(BR(\mathbf{3}) + BR(\mathbf{4}))]_{hetero}$, where the indices "homo" and "hetero" indicate the homochiral (*R*,*R*) and heterochiral (*R*,*S*) complexes with the first indicator assigning the chirality of the BINOL derivative and the second one the chirality of the ester.

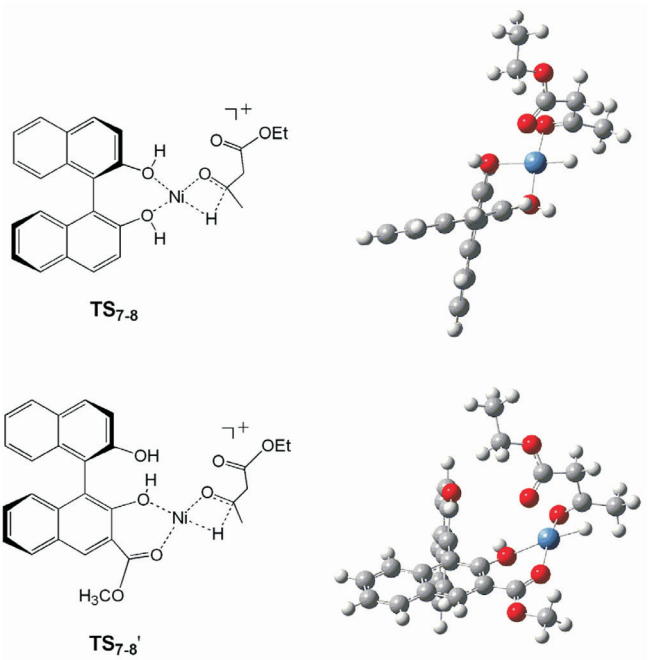

FIG. 5
Optimized geometries of the computed transition structures **TS$_{7\text{-}8}$** and **TS$_{7\text{-}8}$′** for the unsubstituted BINOLato ligand **1** and a monocarboxymethyl derivative serving as a model for ligand **2**

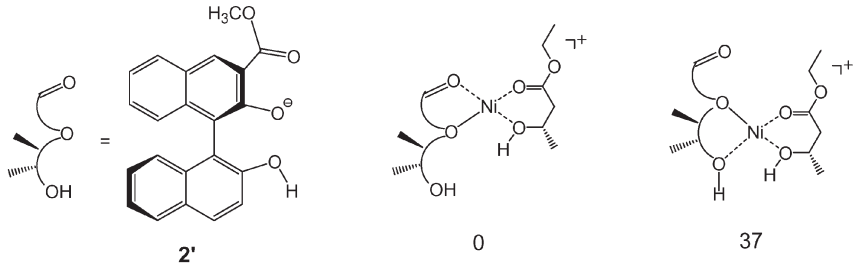

SCHEME 4
Illustration of the calculated most stable isomers for the complexes of [(**2′**)Ni]$^+$ with *S*-ethyl 3-hydroxybutyrate; relative energies are given in kJ/mol

The lack of selectivity observed for the complexes of $[(\mathbf{2})Ni]^+$ with ethyl 3-hydroxybutyrate can be explained by the different binding situation of nickel with the BINOL derivative **2**. Hence, the carbonyl-oxygen of the carboxymethyl moiety binds the Ni center more tightly (37 kJ/mol lower in energy), than the hydroxyl next to the chiral axis (Scheme 4). The occurrence of such an interaction removes the charged metal center from the chiral axis of the BINOL, such that the interaction between the two chiral centers, which is crucial for the chiral discrimination, is largely reduced.

CONCLUSIONS

Nickel(II) complexes between the BINOL derivatives (**1** and **2**) and the chiral esters (**3** and **4**) have been generated upon electrospray ionization and investigated by means of CID. Whereas the complexes with ethyl lactate lead only to the loss of the intact ester ligand, ethyl 3-hydroxybutyrate is dehydrogenated by gaseous $[(\mathbf{1})Ni]^+$ and $[(\mathbf{2})Ni]^+$ ions to yield the corresponding nickel-hydrido cations concomitant with ethyl acetylacetate as a neutral product. In the case of the $[(\mathbf{1})Ni]^+$ cation, this process shows a significant discrimination between the enantiomers of **4** with preferential occurrence of C–H bond activation for the heterochiral variants. In contrast, no enantiodiscrimination is found for the complexes with the ortho-substituted BINOL derivative $[(\mathbf{2})Ni]^+$. The experimental findings provide insights in the structural features, which are able to induce chiral discrimination in gas-phase bond-activation processes. Specifically, the choice of a substrate bearing additional binding sites for the metal center somewhat decreases its reactivity, but increases the stereochemical effect in comparison to aliphatic secondary alcohols. In contrast, introduction of additional chelating moieties on the BINOL frame in compound **2** gives rise to a complex where the two chiral centers are too remote from each other, such that the stereochemical effect vanishes. Therefore it seems worthy to further screen chiral BINOL derivatives, which do not change the complexation site of the metal, while increasing the steric constraints of the complex.

Continuous financial support by the Academy of Sciences of the Czech Republic (Z40550506), the Deutsche Forschungsgemeinschaft, the Fonds der Chemischen Industrie, the Gesellschaft der Freunde der Technischen Universität, and the Grant Agency of the Academy of Sciences of the Czech Republic (KJB400550704) is gratefully acknowledged. X. Zhang thanks the Alexander von Humboldt Foundation for a postdoctoral fellowship. We thank W. Zummack for the synthesis of various substances employed in this study.

REFERENCES AND NOTES

1. a) Brunel J.-M.: *Chem. Rev.* **2005**, *105*, 857; b) Brunel J.-M.: *Chem. Rev.* **2007**, 107, PR1.
2. Splitter J. S., Tureček F. (Eds): *Applications of Mass Spectrometry to Organic Stereochemistry*. VCH, Weinheim 1994.
3. Schalley C. A.: *Int. J. Mass Spectrom.* **2000**, *194*, 11.
4. Speranza M.: *Int. J. Mass Spectrom.* **2004**, *232*, 277.
5. See also: Schröder D., Schwarz H.: *Int. J. Mass Spectrom.* **2004**, *231*, 139.
6. Rochut S., Roithová J., Schröder D., Novara F. R., Schwarz H.: *J. Am. Soc. Mass Spectrom.* **2008**, *19*, 121.
7. Novara F. R., Schröder D., Schwarz H.: *Helv. Chim. Acta* **2007**, *90*, 2274.
8. Novara F. R., Gruene P., Schröder D., Schwarz H.: *Chem. Eur. J.* **2008**, *14*, 5957.
9. Cooks R. G., Wong P. S. H.: *Acc. Chem. Res.* **1998**, *31*, 379.
10. a) Noyori R., Ohkuma T.: *Angew. Chem.* **2001**, *113*, 40; b) Noyori R., Ohkuma T.: *Angew. Chem. Int. Ed.* **2001**, *40*, 40.
11. Roithová J., Schröder D.: *Chem. Eur. J.* **2008**, *14*, 2180.
12. Wipf B., Kupfer E., Bertazzi R., Leuenberger H. G. W.: *Helv. Chim. Acta* **1983**, *66*, 485.
13. Kumar M. R., Prabhakar S., Kumar M. K., Reddy T. J., Vairamani M.: *Rapid Commun. Mass Spectrom.* **2005**, *19*, 113.
14. Davies H. M. L., Huby N. J. S., Cantrell W. R., Olive J. L.: *J. Am. Chem. Soc.* **1993**, *115*, 9468.
15. Schröder D., Weiske T., Schwarz H.: *Int. J. Mass Spectrom.* **2002**, *219*, 729.
16. Calculated using the Chemputer made by M. Winter, University of Sheffield, see: http://winter.group.shef.ac.uk/computer/.
17. a) Schröder D., Schwarz H., Schenk S., Anders E.: *Angew. Chem.* **2003**, *115*, 5241; b) Schröder D., Schwarz H., Schenk S., Anders E.: *Angew. Chem. Int. Ed.* **2003**, *42*, 5087.
18. Schröder D., Engeser M., Brönstrup M., Daniel C., Spandl J., Hartl H.: *Int. J. Mass Spectrom.* **2003**, *228*, 743.
19. Schlangen M., Neugebauer J., Reiher M., Schröder D., Pitarch-Lopez J., Haryono M., Heinemann F. W., Grohmann A., Schwarz H.: *J. Am. Chem. Soc.* **2008**, *130*, 4285.
20. Trage C., Diefenbach M., Schröder D., Schwarz H.: *Chem. Eur. J.* **2006**, *12*, 2454.
21. Gruene P., Trage C., Schröder D., Schwarz H.: *Eur. J. Inorg. Chem.* **2006**, 4546.
22. Schröder D., Engeser M., Schwarz H., Rosenthal E. C. E., Döbler J., Sauer J.: *Inorg. Chem.* **2006**, *45*, 6235.
23. Jagoda-Cwiklik B., Jungwirth P., Rulíšek L., Milko P., Roithová J., Lemaire J., Maitre P., Ortega J. M., Schröder D.: *ChemPhysChem* **2007**, *8*, 1629.
24. Frisch M. J., Trucks G. W., Schlegel H. B., Scuseria G. E., Robb M. A., Cheeseman J. R., Montgomery J. A., Jr., Vreven T., Kudin K. N., Burant J. C., Millam J. M., Iyengar S. S., Tomasi J., Barone V., Mennucci B., Cossi M., Scalmani G., Rega N., Petersson G. A., Nakatsuji H., Hada M., Ehara M., Toyota K., Fukuda R., Hasegawa J., Ishida M., Nakajima T., Honda Y., Kitao O., Nakai H., Klene M., Li X., Knox J. E., Hratchian H. P., Cross J. B., Adamo C., Jaramillo J., Gomperts R., Stratmann R. E., Yazyev O., Austin A. J., Cammi R., Pomelli C., Ochterski J. W., Ayala P. Y., Morokuma K., Voth G. A., Salvador P., Dannenberg J. J., Zakrzewski V. G., Dapprich S., Daniels A. D., Strain M. C., Farkas O., Malick D. K., Rabuck A. D., Raghavachari K., Foresman J. B., Ortiz J. V., Cui Q., Baboul A. G., Clifford S., Cioslowski J., Stefanov B. B., Liu G., Liashenko A., Piskorz P., Komaromi I., Martin R. L., Fox D. J., Keith T., Al-Laham M. A., Peng C. Y., Nanayakkara A.,

Challacombe M., Gill P. M. W., Johnson B., Chen W., Wong M. W., Gonzalez C., Pople J. A.: *Gaussian 03*. Gaussian, Inc., Wallingford, CT 2004.
25. Ehlers A. W., Böhme M., Dapprich S., Gobbi A., Höllwarth A., Jonas V., Köhler K. F, Stegmann R., Veldkamp A., Frenking G.: *Chem. Phys. Lett.* **1993**, *208*, 111.
26. Ma J. C., Dougherty D. A.: *Chem. Rev.* **1997**, *97*, 1303.
27. Diefenbach M., Schwarz H.: *Chem. Eur. J.* **2005**, *11*, 3058.
28. Corral I., Mo O., Yañez M.: *Int. J. Mass Spectrom.* **2006**, *255*, 20.
29. Zocher E., Dietiker R., Chen P.: *J. Am. Chem. Soc.* **2007**, *129*, 2476.
30. For similar consecutive evaporation of two neutral molecules from gaseous metal complexes see: a) Czekay G., Eller K., Schröder D., Schwarz H.: *Angew. Chem.* **1989**, *101*, 1306; b) Czekay G., Eller K., Schröder D., Schwarz H.: *Angew. Chem., Int. Ed. Engl.* **1989**, *28*, 1277.
31. Schröder D., Schwarz H.: *J. Am. Chem. Soc.* **1990**, *112*, 5947.
32. Butschke B., Schlangen M., Schröder D., Schwarz H.: *Helv. Chim. Acta* **2008**, *91*, 1902.
33. Butschke B., Schlangen M., Schröder D., Schwarz H.: *Chem. Eur. J.* **2008**, *14*, 11050.